

4.10 URBAN AND REGIONAL PLANNING APPLICATIONS

Urban and regional planners require nearly continuous acquisition of data to formulate governmental policies and programs. These policies and programs might range from the social, economic, and cultural domain to the context of environmental and natural resource planning. The role of planning agencies is becoming increasingly more complex and is extending to a wider range of activities. Consequently, there is an increased need for these agencies to have timely, accurate, and cost-effective sources of data of various forms. Several of these data needs are well served by visual image interpretation. A key example is land use/land cover mapping, as discussed in Section 4.4. Another example is the use of image interpretation to contribute data for land use suitability evaluation purposes, as outlined in Section 4.16. Here we discuss the utility of visual image interpretation in population estimation, housing quality studies, traffic and parking studies, site selection processes, and urban change detection.

Population estimates can be indirectly obtained through visual image interpretation. Traditionally, the procedure has been to use medium- to large-scale aerial photographs to estimate the number of dwelling units of each housing type in an area (single-family, two-family, multiple-family) and then multiply the number of dwelling units by the average family size per dwelling unit for each housing type. The identification of housing types is based on such criteria as size and shape of buildings, yards, courts, and driveways.

Images from the *Defense Meteorological Satellite Program (DMSP)* (Chapter 6) have been used to examine the earth's urban development from space. One of the DMSP's scanners, the *Operational Linescan System (OLS)*, is sensitive enough to detect low levels of visible and near-IR energy at night. With this sensor, it is possible to detect clouds illuminated by moonlight, plus lights from cities, towns, industrial sites, gas flares, and ephemeral events such as fires and lightning-illuminated clouds (Elvidge et al., 1997). Figure 4.28 is a global example of DMSP nighttime image data (a composite of hundreds of individual scenes). Figure 4.29 shows DMSP data of the eastern United States. The brightness of the light patterns in Figure 4.29 corresponds closely with the population distribution of the eastern United States, as seen in Figure 4.30. Care must be taken when attempting to compare data from different parts of the world. The brightest areas of the earth are the most urbanized, but not necessarily the most populated (compare western Europe with India and China). Nevertheless, DMSP data provide a valuable data source for tracking the growth of the earth's urbanization over time.

Visual image interpretation can also assist in *housing quality studies*. Many environmental factors affecting housing quality can be readily interpreted from aerial and satellite images, whereas others (such as the interior condition of buildings) cannot be directly interpreted. A reasonable estimate of housing quality can usually be obtained through statistical analysis of a limited, carefully selected set of environmental quality factors. Environmental factors that are



Figure 4-28 Earth lights at night as sensed by the Defense Meteorological Satellite Program Operational Linescan System. (Courtesy NOAA.)

interpretable from aerial photographs and that have been found to be useful in housing quality studies include house size, lot size, building density, building setback, street width and condition, curb and sidewalk condition, driveway presence/absence, garage presence/absence, vegetation quality, yard and open space maintenance, proximity to parkland, and proximity to industrial land use. Large-scale panchromatic photography has typically been used for housing quality studies. However, large- to medium-scale color infrared film has been shown to be superior in evaluating vegetation condition (lawns, shrubs, and trees).

Visual image interpretation can assist in *traffic and parking studies*. Traditional on-the-ground vehicle counts show the number of vehicles passing a few selected points over a period of time. An aerial image shows the distribution of vehicles over space at an instant of time. Vehicle spacings—and thus areas of congestion—can be evaluated by viewing such photographs. Average vehicle speeds can be determined when the image scale and time interval between exposures of overlapping photographs are known. The number and spatial distribution of vehicles parked in open-air lots and streets can be inventoried from aerial images. Not all vehicles in urban areas are visible on aerial images, however. Vehicles in tunnels and enclosed parking will obviously not be visible. In an area of tall buildings, streets near the edges of photographs may be hidden from view because of the radial relief displacement of the buildings. In addition, it may be difficult to discern vehicles in shadow areas on films of high contrast.

Visual image interpretation can assist in various location and siting problems, such as transportation route location, sanitary landfill site selection, power plant siting, commercial site selection, and transmission line location. The same general decision-making process is followed in each of these selection processes. First the factors to be assessed in the route/site selection process are determined. Natural and cultural features plus various economic, social, and political factors are considered. Then data files containing information on these factors are assembled and alternative routes/sites are analyzed and the final route/site is selected. Visual image interpretation has been used to collect much of the natural and cultural data dealing with topography, geology, soils, potential construction materials, vegetation, land use, wetland location, historical/archaeological sites, and natural hazards (earthquakes, landslides, floods, volcanoes, and tsunamis). Various methods for obtaining such natural and cultural data through visual image interpretation are described elsewhere in this chapter. The task of analyzing the data is greatly facilitated by the use of a GIS.

Urban change detection mapping and analysis can be facilitated through the interpretation of multirate aerial and satellite images, such as the photographs shown in Figure 4.31, which illustrate the changes in an urban fringe area over a period of 53 years. The 1937 photograph (*a*) shows the area to be entirely agricultural land. The 1955 photograph (*b*) shows that a “beltline” highway has been constructed across the top of the area and that a gravel pit has begun operation in a glacial outwash plain at lower left. The 1968 photograph (*c*) shows that commercial development has begun at upper left and that extensive single-family housing development has begun at lower right. A



Figure 4.29 Defense Meteorological Satellite Program nighttime image of the eastern United States, 1981, 0.4- to 1.1- μm band. (Courtesy U.S. Air Force and NOAA.)

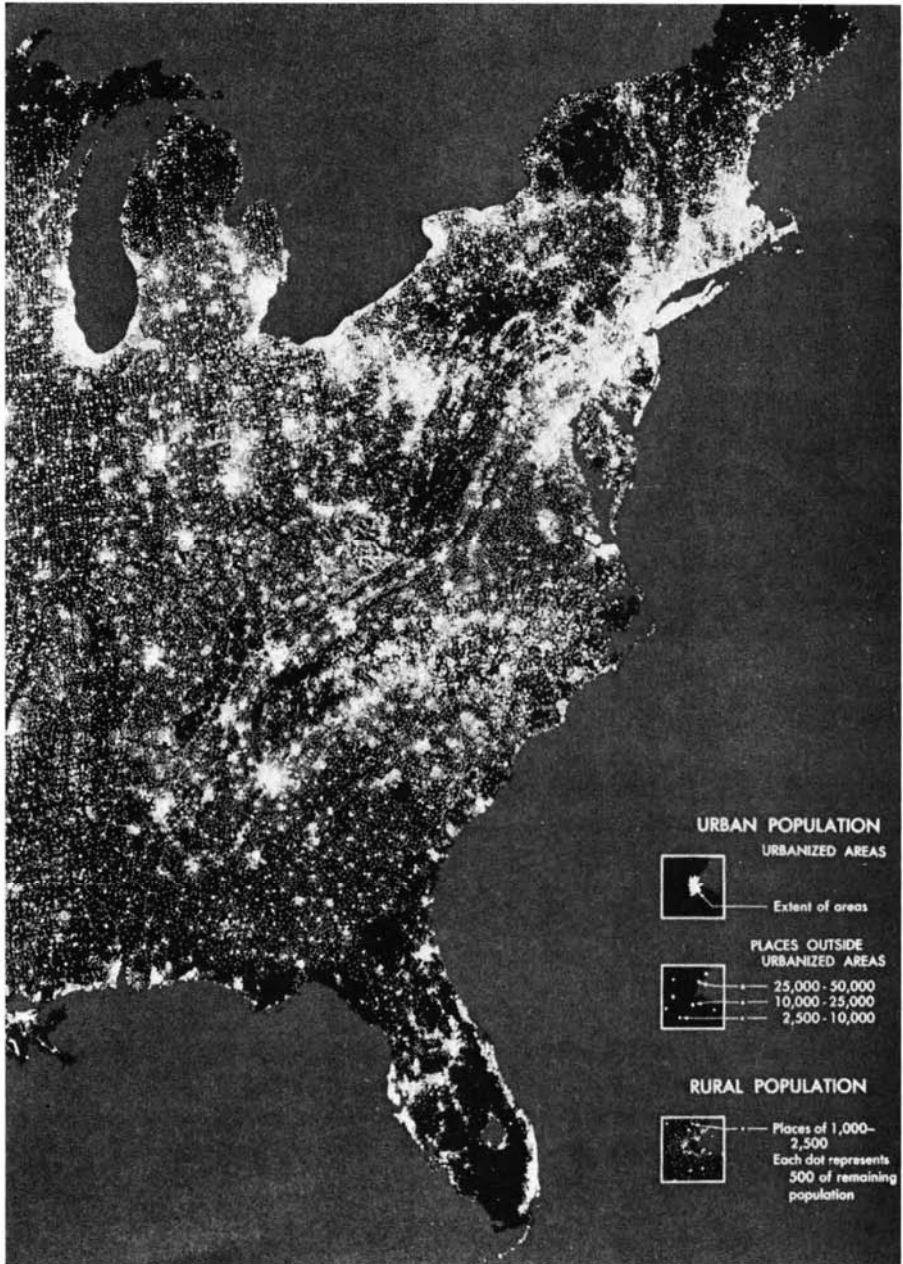


Figure 4.30 Map showing eastern U.S. population distribution in 1970. Population is proportional to brightness (see map legend). (U.S. Bureau of Census map.)



Figure 4.31 Multidate aerial photographs illustrating urban change, southwest Madison, WI (scale 1:20,000): (a) 1937; (b) 1955; (c) 1968; (d) 1990. [(a-c) USDA-ASCS photos. (d) Courtesy Dane County Regional Planning Commission.]



Figure 4.31 (Continued)

school has been constructed at lower center and the gravel pit continues operation. The 1990 photograph (*d*) shows that the commercial and single-family development has continued. Multiple-family housing units have been constructed at left. The gravel pit site is now a city park that was a sanitary landfill site for a number of years between the dates of photographs (*c*) and (*d*).

Plate 10 illustrates the use of satellite data for urban change detection. These Landsat images (Chapter 6) dramatically illustrate population growth in the Las Vegas metropolitan area (the fastest growing metropolitan area in the United States) over a 28-year period. The estimated population in the area shown was 300,000 in 1972 (*a*), and 1,425,000 in 2000 (*b*).

Visual image interpretation for urban change detection and analysis can be facilitated through the use of a Digital Transfer Scope (Section 4.3) as an aid in comparing images of two different dates or an image with a map.

4.11 WETLAND MAPPING

The value of the world's wetland systems has gained increased recognition. Wetlands contribute to a healthy environment in many ways. They act to retain water during dry periods, thus keeping the water table high and relatively stable. During periods of flooding, they act to reduce flood levels and to trap suspended solids and attached nutrients. Thus, streams flowing into lakes by way of wetland areas will transport fewer suspended solids and nutrients to the lakes than if they flow directly into the lakes. The removal of such wetland systems because of urbanization or other factors typically causes lake water quality to worsen. In addition, wetlands are important feeding, breeding, and drinking areas for wildlife and provide a stopping place and refuge for waterfowl. As with any natural habitat, wetlands are important in supporting species diversity and have a complex and important food web. Scientific values of wetlands include a record of biological and botanical events of the past, a place to study biological relationships, and a place for teaching. It is especially easy to obtain a feel for the biological world by studying a wetland. Other human uses include low intensity recreation and esthetic enjoyment.

Accompanying the increased interest in wetlands has been an increased emphasis on inventorying. The design of any particular wetland inventory is dependent on the objectives to be met by that inventory. Thus, a clearly defined purpose must be established before the inventory is even contemplated. Wetland inventories may be designed to meet the general needs of a broad range of users or to fulfill a very specific purpose for a particular application. Multipurpose and single-purpose inventories are both valid ways of obtaining wetland information, but the former minimizes duplication of effort. To perform a wetlands inventory, a classification system must be devised that will provide the information necessary to the inventory users. The system should be based primarily on enduring wetland characteristics so that the inventory does not become outdated too quickly, but the classification should also accommodate user

information requirements for ephemeral wetland characteristics. In addition, the inventory system must provide a detailed description of specifically what is considered to be a wetland. If the wetland definition used for various "wetland maps" is not clearly stated, then it is not possible to tell if apparent wetland changes noted between maps of different ages result from actual wetland changes or are due to differences in concepts of what is considered a wetland.

At the federal level in the United States, four principal agencies are involved with wetland identification and delineation: (1) the Environmental Protection Agency, (2) the Army Corps of Engineers, (3) the Natural Resources Conservation Service, and (4) the Fish and Wildlife Service. The Environmental Protection Agency is concerned principally with water quality, the Army Corps of Engineers is concerned principally with navigable water issues that may be related to wetlands, the Natural Resources Conservation Service is concerned principally with identifying and mapping wetlands, and the Fish and Wildlife Service is principally interested in the use of wetlands for wildlife habitat. In 1989, these four agencies produced a *Federal Manual for Identifying and Delineating Jurisdictional Wetlands* (Federal Interagency Committee for Wetland Delineation, 1989), which provides a common basis for identifying and delineating wetlands. There is general agreement on the three basic elements for identifying wetlands: (1) hydrophytic vegetation, (2) hydric soils, and (3) wetland hydrology. *Hydrophytic vegetation* is defined as macrophytic plant life growing in water, soil, or substrate that is at least periodically deficient in oxygen as a result of excessive water content. *Hydric soils* are defined as soils that are saturated, flooded, or ponded long enough during the growing season to develop anaerobic (lacking free oxygen) conditions in the upper part. In general, hydric soils are flooded, ponded, or saturated for 1 week or more during the period when soil temperatures are above biologic zero (5°C) and usually support hydrophytic vegetation. *Wetland hydrology* refers to conditions of permanent or periodic inundation, or soil saturation to the surface, at least seasonally, hydrologic conditions that are the driving forces behind wetland formation. Numerous factors influence the wetness of an area, including precipitation, stratigraphy, topography, soil permeability, and plant cover. All wetlands typically have at least a seasonal abundance of water that may come from direct precipitation, overbank flooding, surface water runoff resulting from precipitation or snow melt, groundwater discharge, or tidal flooding.

Color infrared photography has been the preferred film type for wetlands image interpretation. It provides interpreters with a high level of contrast in image tone and color between wetland and nonwetland environments, and moist soil spectral reflectance patterns contrast more distinctively with less moist soils on color infrared film than on panchromatic or normal color films. Other multiband image types (e.g., multispectral scanners, hyperspectral scanners) can also be used, but should include at least one visible band and one near-infrared band.

An example of wetland mapping is shown in Figures 4.32 and 4.33. Figure 4.32 is a 6.7× enlargement of a color infrared airphoto that was used for



Figure 4.32 Black and white copy of a color infrared aerial photograph of Sheboygan Marsh, WI. Scale 1:9000 (enlarged 6.7 times from 1:60,000). Grid ticks appearing in image are from a reseau grid included in camera focal plane. (NASA image.)



Figure 4.33 Vegetation classes in Sheboygan Marsh (scale 1:9000): W = open water, D = deep water emergents, E = shallow water emergents, C = cattail (solid stand), O = sedges and grasses, R = reed canary grass (solid stand), M = mixed wetland vegetation, S = shrubs, L = lowland conifer forest.

TABLE 4.13 Airphoto Interpretation Key to Vegetation Classes in Sheboygan Marsh for Use with Late-Spring 1: 60,000 Color Infrared Film

Map Symbol (Figure 4.33)	Class Definition and Airphoto Interpretation Key
W	<i>Open water:</i> Areas of open water produce a dark blue image. The dark color and uniform smooth texture of the open water are in distinct contrast with the lighter tones of the surrounding vegetation.
D	<i>Deep water emergents:</i> These exist in water depths of 0.15–0.45 m or more and consist predominantly of cattail (<i>Typha latifolia</i> , <i>T. augustifolia</i>), burreed (<i>Sparganium eurycarpum</i>), and sometimes reedgrass (<i>Phragmites communis</i>). These species, when interspersed with water, form an image made up of a dull bluish color with soft texture, a tone produced by background reflectance of water blending with the vegetation reflectance. This subcommunity is sometimes interspersed with shallow water emergents.
E	<i>Shallow water emergents:</i> These consist of a mixture of such wetland species as cattail (<i>T. latifolia</i> , <i>T. augustifolia</i>), arrowhead (<i>Sagittaria latifolia</i>), water plantain (<i>Alisma plantago-aquatica</i>), burreed (<i>S. eurycarpum</i>), and several sedge species (<i>Carex lacustris</i> , <i>C. rostrata</i> , <i>C. stricta</i> , <i>C. aquatilis</i>) in water depths of 0.15 m or less. A medium bluish tone is produced that is lighter than the deep water areas.
C	<i>Cattail-solid stand:</i> This consists of solid stands of cattail (<i>T. latifolia</i> , <i>T. augustifolia</i>) that appear as mottled white patches in water ranging in depth from 0.10 to 0.75 m.
O	<i>Sedges and grasses:</i> The main components of a sedge meadow, sedges (<i>C. lacustris</i> , <i>C. rostrata</i> , <i>C. stricta</i> , <i>C. aquatilis</i>) and grasses (<i>Spartina</i> sp, <i>Phragmites</i> sp, <i>Calamagrostis</i> sp) are generally interspersed with small depressions of shallow water that together produce a continuous pattern of bluish water color intermixed with small white blotches.
R	<i>Reed canary grass-solid stand:</i> Reed canary grass appears as a uniform vegetation type that produces a bright white tone on the image. Reed canary grass occurs in small irregular patches and as linear features along stream banks. It is often difficult to differentiate from sedges and grasses because of the almost identical tones produced. Large areas of the species that were planted for marsh hay often retain their unnatural rectangular boundaries.
M	<i>Mixed wetland vegetation:</i> This consists primarily of sedges (<i>C. rostrata</i> , <i>C. stricta</i> , <i>C. lacustris</i>), forbs (marsh dock, <i>Rumex brittanica</i> ; marsh bellflower, <i>Campanula aparinoides</i> ; and marsh bedstraw, <i>Galium trifidum</i>), grasses (bluejoint, <i>Calamagrostis canadensis</i>), and cord grass (<i>Sparganium</i> sp). This community produces an interlacing pattern of magenta tones, light blues, and white colors, indicating the mixture of the component species.
S	<i>Shrubs:</i> This consists of buttonbush (<i>Cephalanthus occidentalis</i> L.), alder (<i>Alnus rugosa</i>), willow (<i>Salix interior</i> , <i>S. petiolaris</i> , <i>S. bebbiana</i>), and red osier dogwood (<i>Cornus stolonifera</i>). Shrubby areas have an intense magenta tone with coarse texture.
L	<i>Lowland conifer forest:</i> This consists, at this site, primarily of tamarack (<i>Larix laricina</i>) and white cedar (<i>Thuja occidentalis</i>) that display a deep mauve tone with considerable texture.

wetland vegetation mapping at an original scale of 1:60,000. The vegetation classification system and airphoto interpretation key are shown in Table 4.13. The wetland vegetation map (Figure 4.33) shows the vegetation in this scene grouped into nine classes. The smallest units mapped at the original scale of 1:60,000 are a few distinctive stands of reed canary grass and cattails about $\frac{1}{3}$ ha in size. Most of the units mapped are much larger.

Another example of wetland mapping can be seen in Plate 28, which illustrates multitemporal data merging as an aid in mapping invasive plant species, in this case reed canary grass.

At the federal level, the U.S. Fish and Wildlife Service is responsible for a National Wetlands Inventory that produces information on the characteristics, extent, and status of the nation's wetlands and deep water habitats. This information is used by federal, state, and local agencies, academic institutions, the U.S. Congress, and the private sector. As of 2002, the National Wetlands Inventory had mapped 90 percent of the lower 48 states, and 34 percent of Alaska. About 44 percent of the lower 48 states, and 13 percent of Alaska had been digitized. Congressional mandates require the production of status and trends reports at 10-year intervals. Updates to map and digital coverage are available on the Internet at: <http://www.nwi.fws.gov>.

4.12 WILDLIFE ECOLOGY APPLICATIONS

The term *wildlife* refers to animals that live in a wild, undomesticated state. *Wildlife ecology* is concerned with the interactions between wildlife and their environment. Related activities are *wildlife conservation* and *wildlife management*. Two aspects of wildlife ecology for which visual image interpretation can most readily provide useful information are wildlife habitat mapping and wildlife censusing.

A *wildlife habitat* provides the necessary combination of climate, substrate, and vegetation that each animal species requires. Within a habitat, the functional area that an animal occupies is referred to as its *niche*. Throughout evolution, various species of animals have adapted to various combinations of physical factors and vegetation. The adaptations of each species suit it to a particular habitat and rule out its use of other places. The number and type of animals that can be supported in a habitat are determined by the amount and distribution of food, shelter, and water in relation to the mobility of the animal. By determining the food, shelter, and water characteristics of a particular area, general inferences can be drawn about the ability of that area to meet the habitat requirements of different wildlife species. Because these requirements involve many natural factors, the image interpretation techniques described elsewhere in this chapter for mapping land cover, soil, forests, wetlands, and water resources are applicable to

wildlife habitat analysis. Also, delineation of the “edges” between various landscape features is an important aspect of habitat analysis. Often, the interpreted habitat characteristics are incorporated in GIS-based modeling of the relationship between the habitat and the number and behavior of various species.

Figure 4.34 illustrates wildlife habitat mapping. This figure shows the Sheboygan Marsh, which was also shown in Figure 4.32 for the purpose of illustrating wetland vegetation mapping. In Figure 4.34, the nine vegetation classes shown in Figure 4.33 have been grouped into five wildlife habitat types, as follows: (1) *open water*, (2) *aquatic vegetation* (cattail, burreed, and reed grass), (3) *sedge meadow* (sedges and grasses), (4) *shrubs* (alder, willow, and dogwood), and (5) *lowland conifer forest* (tamarack and white cedar). Each of these five habitat types supports a significantly different population of mammals, birds, and fish. For example, a careful examination of the “aquatic vegetation” habitat area of Figure 4.34 on the original color infrared transparency (1:60,000) reveals that there are more than 100 white spots on the photograph, each surrounded by a dark area. Each of these white spots is a muskrat hut. Within the area of this photograph, muskrat huts can be found only in the area identified as aquatic vegetation habitat.

Wildlife censusing can be accomplished by ground surveys, aerial visual observations, or aerial imaging. Ground surveys rely on statistical sampling techniques and are often tedious, time consuming, and inaccurate. Many of the wildlife areas to be sampled are often nearly inaccessible on the ground. Aerial visual observations involve attempting to count the number of individuals of a species while flying over a survey area. Although this can be a low cost and relatively rapid type of survey, there are many problems involved. Aerial visual observations require quick decisions on the part of the observer regarding numbers, species composition, and percentages of various age and sex classes. Aggregations of mammals or birds may be too large for accurate counting in the brief time period available. In addition, low-flying aircraft almost invariably disturb wildlife, with much of the population taking cover before being counted.

Vertical aerial photography has been the best method of accurately censusing many wildlife populations. If the mammals or birds are not disturbed by the aircraft, the airphotos will permit very accurate counts to be undertaken. In addition, normal patterns of spatial distributions of individuals within groups will be apparent. Aerial photographs provide a permanent record that can be examined any number of times. Prolonged study of the photographs may reveal information that could not have been otherwise understood.

A variety of mammals and birds have been successfully censused using vertical aerial photography, including moose, elephants, whales, elk, sheep,



Figure 4.34 Wildlife habitat types in Sheboygan Marsh (scale 1:9000): W = open water, AV = aquatic vegetation, SM = sedge meadow, S = shrubs, LF = lowland conifer forest.

deer, antelope, sea lions, caribou, beavers, seals, geese, ducks, flamingos, gulls, oyster catchers, and penguins. Vertical aerial photography obviously cannot be used to census all wildlife populations. Only those that frequent relatively open areas during daylight hours can be counted. (Thermal scanning can be used to detect large animals in open areas.)

Wildlife censusing also requires that individual animals be large enough to be resolved on the photographs. A scale not smaller than 1:8000 is recommended for large mammals such as elk, whereas scales as large as 1:3000 should be used for smaller mammals such as sheep, deer, and antelope. A critical factor is the tonal contrast between the animal and its surroundings. For example, flocks of snow geese (large white birds) can be identified at a scale of 1:12,000 against a dark background. Individual birds are identifiable at scales of 1:6000 and larger.

In Figure 4.35, snow geese appear as white dots against a darker water background in the Bosque del Apache National Wildlife Refuge in New Mexico, where as many as 45,000 snow geese visit during their migrations.

Dark-colored wildlife species often can be discerned better in the winter against a snow or ice background than in the summer with a soil, vegetation, or water background. This is also the time of year when many species tend to band together and leaves have fallen from deciduous trees, making censusing possible even in certain kinds of forests. Special film-filter combinations can be selected to maximize the contrast.

The counting of individual animals on aerial images may present a problem when large numbers are present. Transparent grid overlays are often used as an aid in estimating numbers. Aerial images can also be used to stratify population densities (individuals per unit area) for use in stratified sampling techniques. Alternatively, aerial images not already in digital form can be digitized (via image scanning) and digital image processing techniques used to automatically "count" individuals.

Figure 4.36 shows a prairie dog colony on a plateau in South Dakota. Prairie dogs feed upon grasses and broad-leaved plants and construct burrows with mounded entrances. They disturb the ground in the vicinity of the colony, making the area susceptible to invasion by plants that exist in disturbed areas. The lighter toned area on the plateau in the center of the photograph is covered by such vegetation (mostly forbs) and the surrounding darker toned area is covered by native prairie grass. Each white spot in this lighter toned area is the bare soil associated with one prairie dog mound.

Figure 4.37 shows a large group of beluga whales (small white whales) that have congregated in an arctic estuarine environment principally for the purpose of calving. At the image scales shown here, it is possible to determine the number and characteristics of individual whales and to measure their lengths. On the full 230 × 230-mm aerial photograph from which Figure 4.37 was rephotographed, a total of about 1600 individual whales were counted. At

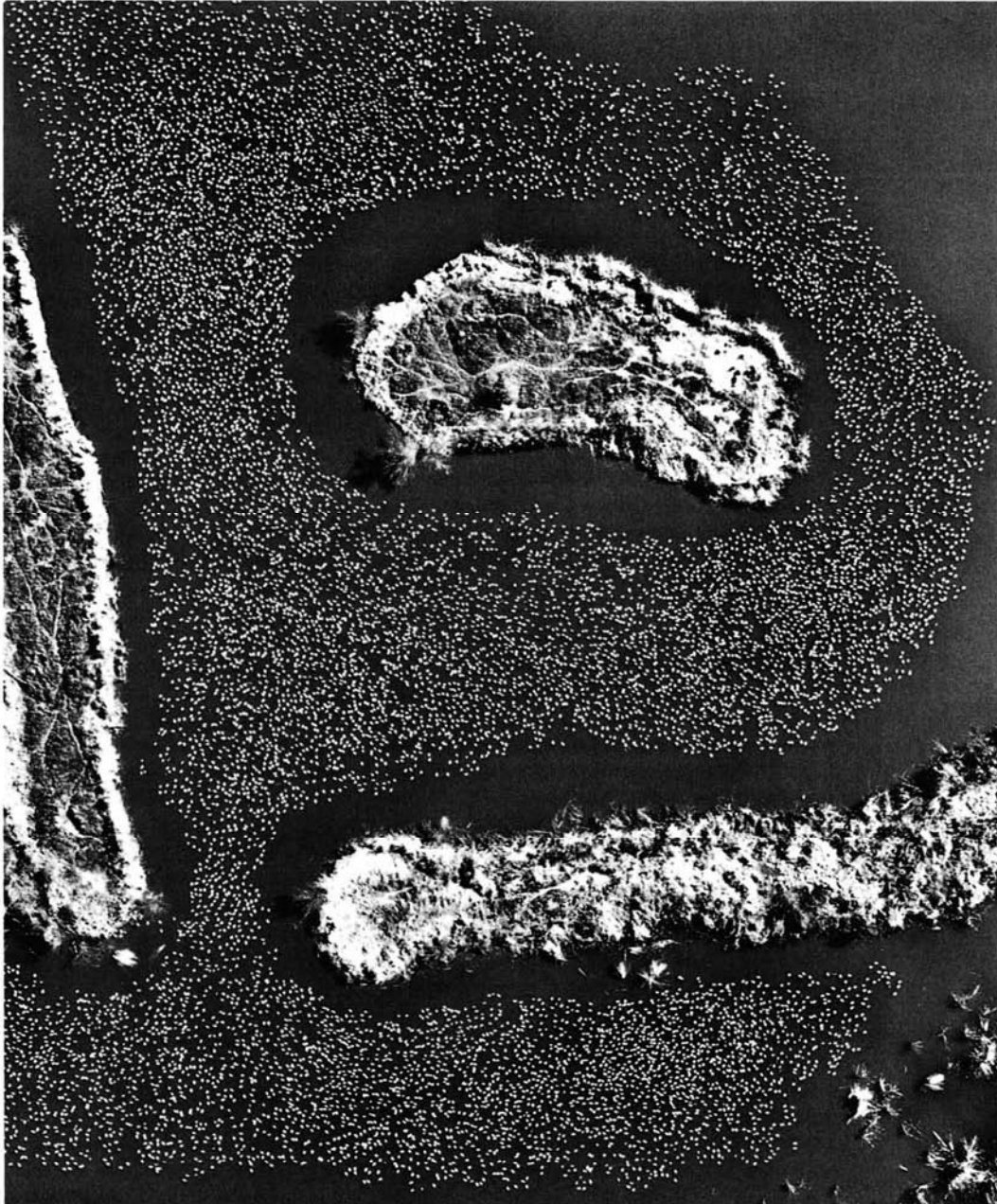


Figure 4.35 Large group of snow geese on water, Bosque del Apache National Wildlife Refuge, NM (black and white copy of a portion of a 230 × 230 mm color infrared aerial photograph). Late November. Approximate scale 1:1000. (Courtesy Kodak Aerial Services and U.S. Fish and Wildlife Service.)

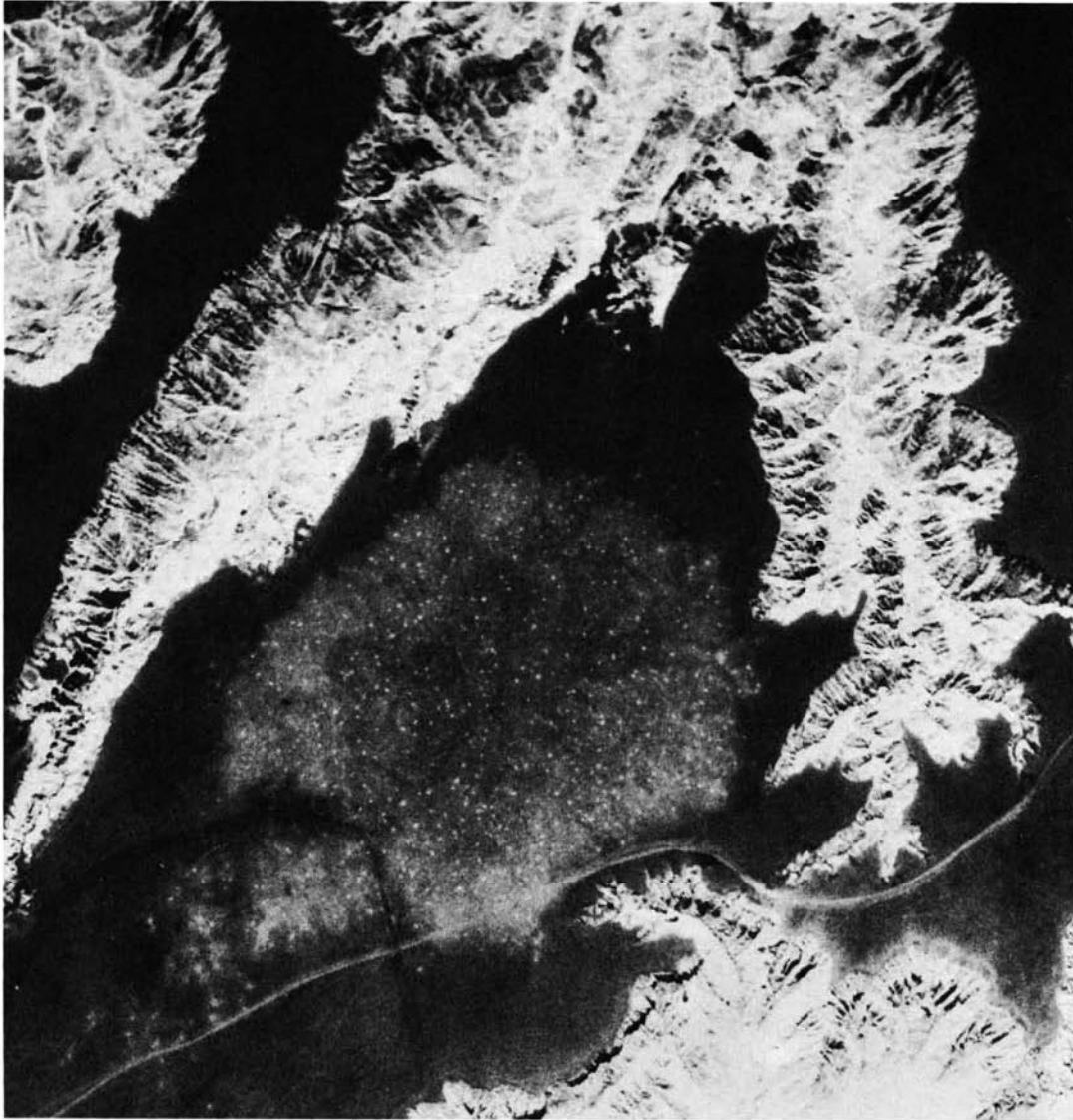


Figure 4.36 Prairie dog colony, Cuny Table, SD. Scale 1:9000. Panchromatic film with a red filter. (Courtesy Remote Sensing Institute, South Dakota State University.)

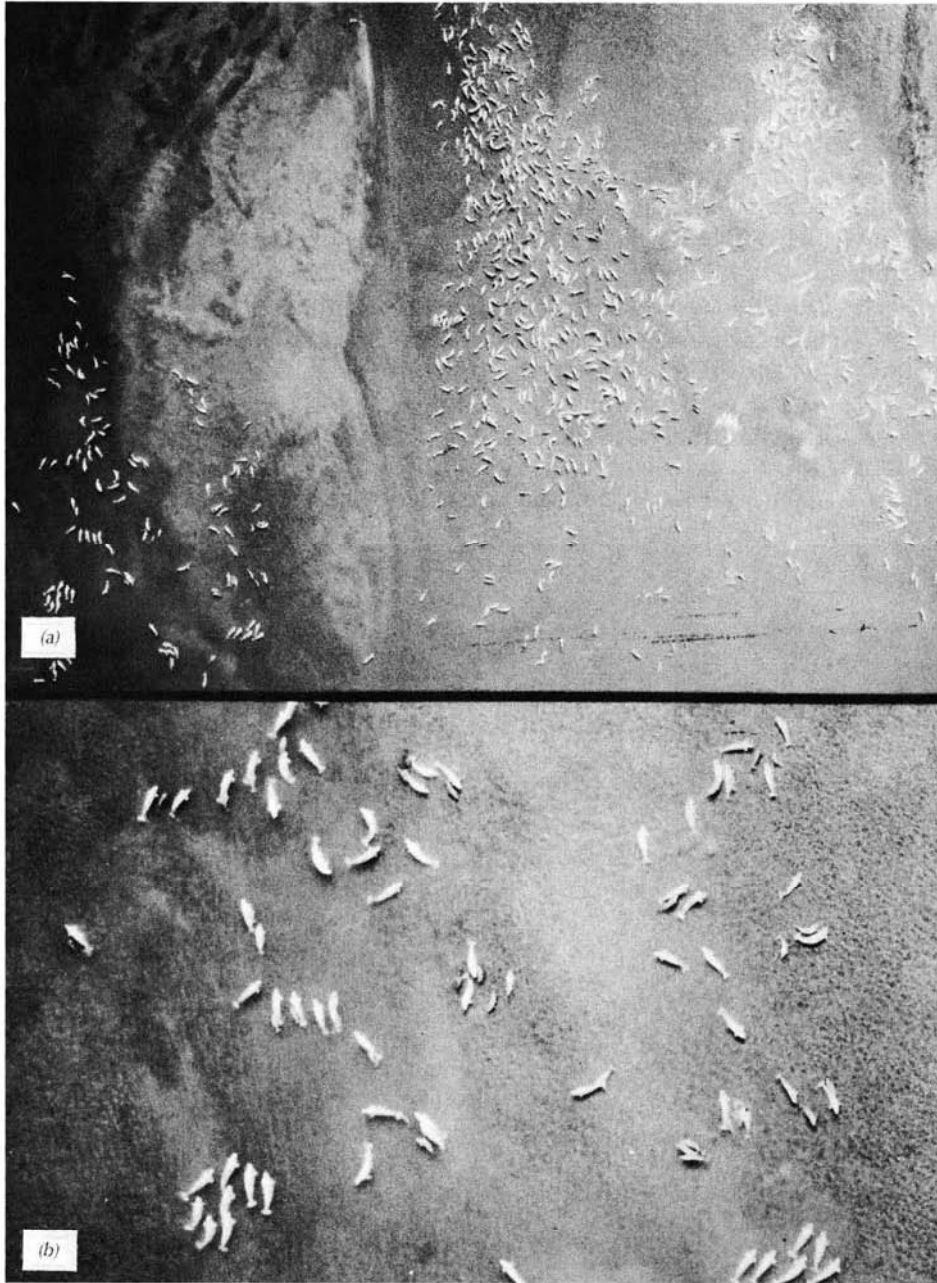


Figure 4.37 Large group of beluga whales, Cunningham Inlet, Somerset Island, northern Canada (black and white copy of photograph taken with Kodak Water Penetration Color Film, SO-224): (a) 1:2,400; (b) 1:800. (b) is a 3 times enlargement of the lower left portion of (a). (Courtesy J. D. Heyland, Metcalfe, Ontario.)

the original film scale of 1:2000, the average adult length was measured as 4 m and the average calf length was measured as 2 m. Numerous adults with calves can be seen, especially in the enlargement (Figure 4.37b). “Bachelor groups” of eight and six males can be seen at the lower left and lower right of Figure 4.37b.

4.13 ARCHAEOLOGICAL APPLICATIONS

Archaeology is concerned with the scientific study of historic or prehistoric peoples by analysis of the remains of their existence, especially those remains that have been discovered through earth excavation.

The earliest archaeological investigations dealt with obvious monuments of earlier societies. The existence of these sites was often known from histori-



Figure 4.38 Vertical photomosaic showing Nazca Lines, Peru. (From Kosok, 1965. Courtesy Long Island University Press.)

cal accounts. Visual image interpretation has proven particularly useful in locating sites whose existence has been lost to history. Both surface and subsurface features of interest to archaeologists have been detected using visual image interpretation.

Surface features include visible ruins, mounds, rock piles, and various other surface markings. Examples of visible ruins are rock structures such as Stonehenge (England), castles (throughout Europe), and Indian dwellings in the southwestern United States. Examples of mounds are the bird-shaped and serpent-shaped Indian mounds of the Midwestern United States. Examples of rock structures are the various medicine wheels such as the Bighorn Medicine Wheel in Wyoming and the Moose Mountain Medicine Wheel in Saskatchewan. Other surface markings include Indian pictographs and the ancient Nazca Lines in Peru.

Figure 4.38 shows the Nazca Lines. They are estimated to have been made between 1300 and 2200 years ago and cover an area of about 500 km². Many geometric shapes have been found, as well as narrow straight lines that extend for as long as 8 km. They were made by clearing away literally millions of rocks to expose the lighter toned ground beneath. The cleared rocks were piled around the outer boundaries of the "lines." These markings were first noticed from the air during the 1920s. At that time, it was hypothesized that they formed a gigantic astronomical calendar, a belief still held by some scientists. The definite reason for their construction remains unknown.

Subsurface archaeological features include buried ruins of buildings, ditches, canals, and roads. When such features are covered by agricultural fields or native vegetation, they may be revealed on aerial or satellite images by tonal anomalies resulting from subtle differences in soil moisture or crop growth. On occasion, such features have been revealed by ephemeral differences in frost patterns.

Figure 4.39 shows the site of the ancient city of Spina on the Po River delta in Italy. Spina flourished during the fifth century B.C. and later became a "lost" city whose very existence was doubted by many. An extensive search for Spina ended in 1956 when it was identified on aerial photographs by an Italian archaeologist. Ancient Spina was a city of canals and waterways. The dark-toned linear features in Figure 4.39 are areas of dense vegetation growing in wet soils at the former location of the canals. The lighter toned rectangular areas are sparse vegetation over sand and the rubble of brick foundations. The light-toned linear features that run diagonally across this photograph are present-day drainage ditches.

The sites of more than a thousand Roman villas have been discovered in northern France through the use of 35-mm aerial photography. The buildings were destroyed in the third century A.D., but their foundation materials remain in the soil. In Figure 4.40, we see the villa foundation because of



Figure 4.39 Oblique aerial photograph showing site of the ancient city of Spina, Italy. (Courtesy Fotoaerea Valvasori, Ravenna, Italy.)

differences in crop vigor. The area shown in this figure has recently been converted from pasture to cropland. In the early years following such conversion, farmers apply little or no fertilizer to the fields. The cereal crops over the foundation materials are light toned owing to both the lack of fertilizer and a period of drought prior to the date of photography. The crops are darker toned over the remainder of the field. The main building (in the foreground) was 95×60 m.

Figure 4.41, an IKONOS image (Chapter 6) of the pyramids and sphinx at Giza, Egypt, shows the level of detail that can be seen in high resolution space images of archaeological sites. Shown at *a* is the Great Pyramid of Khufu. At

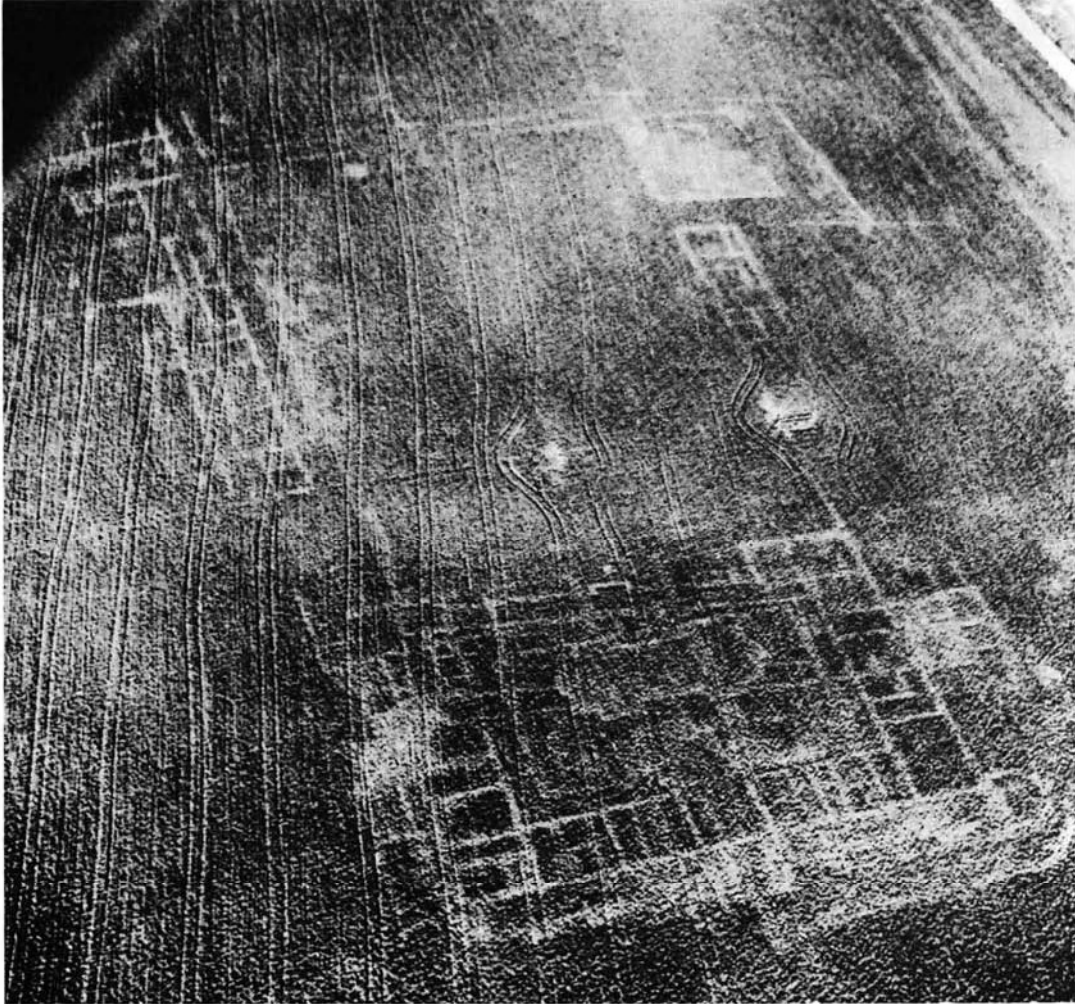


Figure 4.40 Oblique 35-mm airphoto of a cereal crop field in northern France. Differences in crop vigor reveal the foundation of a Roman villa. (Photograph by R. Agache. From Wilson, 1975. Courtesy The Council for British Archaeology, London.)

b is the Pyramid of Khafre; at *c* is the Pyramid of Menkaure, and just left of *d* is the Great Sphinx. The numerous small rectangular features left and right of the Great Pyramid are flat-topped funerary structures called “mastabas.” The pyramids and sphinx were built about 4500 years ago. The length of each side of the Great Pyramid averages 230 m at its base, and the four sides are accurately oriented in the four cardinal directions (north, east, south, and west). The Great Sphinx is 73 m long, is carved out of limestone bedrock, and faces the rising sun.



Figure 4.41 IKONOS image, pyramids and sphinx at Giza, Egypt. Scale 1:12,600. North is to the bottom of the page. (Courtesy Space Imaging.)

4.14 ENVIRONMENTAL ASSESSMENT

Many human activities produce potentially adverse environmental effects. Examples include the construction and operation of highways, railroads, pipelines, airports, industrial sites, power plants, and transmission lines; subdivision and commercial developments; sanitary landfill and hazardous waste disposal operations; and timber harvesting and strip mining operations.

Dating as far back as 1969, the *National Environmental Policy Act* (NEPA) established as national policy the creation and maintenance of conditions that encourage harmony between people and their environment and minimize environmental degradation. This act requires that *environmental impact statements* be prepared for any federal action having significant impact on the environment. The key items to be evaluated in an environmental impact statement are (1) the environmental impact of the proposed action; (2) any adverse environmental effects that cannot be avoided should the action be implemented; (3) alternatives to the proposed action; (4) the relationship between local short term uses of the environment and the maintenance and enhancement of long term productivity; and (5) any irreversible and irretrievable commitments of resources that would be involved in the proposed action should it be implemented. Since the passage of NEPA, many other federal and state laws have been passed with environmental assessment as a primary component.

Environmental assessments involve, at a minimum, comprehensive inventory of physiographic, geologic, soil, cultural, vegetative, wildlife, watershed, and airshed conditions. Such assessments will typically draw on expertise of persons from many areas such as civil engineering, forestry, landscape architecture, land planning, geography, geology, archaeology, environmental economics, rural sociology, ecology, seismology, soils engineering, pedology, botany, biology, zoology, hydrology, water chemistry, aquatic biology, environmental engineering, meteorology, air chemistry, and air pollution engineering. Many of the remote sensing and image interpretation techniques set forth in this book can be utilized to assist in the conduct of such assessments. Overall, the applications of remote sensing in environmental monitoring and assessment are virtually limitless, ranging from environmental impact assessment to emergency response planning, landfill monitoring, permitting and enforcement, and natural disaster mitigation, to name but a few.

Effectively "real-time" imaging is used in such applications as responding to the spillage of hazardous materials. Such images are used to determine the extent and location of visible spillage and release, vegetation damage, and threats to natural drainage and human welfare. On the other hand, historical images are often used to conduct intensive site analyses of waste sites, augmenting these with current images when necessary. These analyses may include characterizing changes in surface drainage conditions through time; identifying the location of landfills, waste treatment ponds, and lagoons and their subsequent burial and abandonment; and detecting and identifying drums containing waste materials. Also, image interpretation may be used to help locate potential sites for drilling and sampling of hazardous wastes.

Figure 4.42 shows a plume of chlorine gas resulting from a train derailment. When such incidents occur, there is immediate need to assess downwind susceptibility of human exposure and the other potential impacts of the event. When available, remote sensing imagery and numerous forms of GIS



Figure 4.42 Low altitude, oblique aerial photograph of chlorine spill resulting from train derailment near Alberton, MT. (Courtesy RMP Systems.)

data are used in conjunction with ancillary ground information (such as wind speed and direction) to develop emergency evacuation and response plans in the general vicinity of the incident. In the specific case of Figure 4.42, the GIS and remote sensing initiated for immediate response was also very useful and important for the longer term monitoring of the spill site. Thus, the GIS established for the response was also useful in monitoring and change detection, as would be the case with many similar applications.

Figure 4.43 shows an oil spill in Bull Run, near Manassas, Virginia. Several thousand barrels of oil entered a nearby creek and then flowed into the connecting river and a reservoir. Several oil containment booms, clearly visible in Figure 4.43, were placed across the run to entrap the oil and facilitate cleanup efforts. Aerial photographs taken over the next few days followed the path of the oil spill movement. The photographs guided the on-scene coordinator in selecting locations for containment booms and pinpointing areas of oil accumulation. Subsequent photographs verified the success of the containment and cleanup of the spill. An example of a radar image showing an oil slick in the Mediterranean Sea can be seen in Figure 8.44.

Large-scale airphotos have been used in such applications as the identification of failing septic systems. The principal manifestations of septic system



Figure 4.43 Aerial photograph of an oil spill on Bull Run, near Manassas, Virginia. Note the series of booms placed across the river to entrap the oil (the flow of water is from right to left in this photograph). (Courtesy EPA Environmental Photographic Interpretation Center.)

failure are typically the upward or lateral movement of partially treated or untreated wastewater toward the soil surface. As the effluent moves upward and approaches the ground surface, the large amount of nutrients in the effluent causes enhanced growth in the vegetation directly above it. When the effluent reaches the surface, the overabundance of nutrients, coupled with an imbalance in the soil's air-water ratio, causes the vegetation to become stressed and eventually die. Finally, the effluent surfaces and either stands on the ground surface or flows downslope, often manifesting the same growth-stress-death pattern as it moves. Both normal color and color infrared photographs at a scale of around 1:8000 have been used for the detection of such situations (Evans, 1982). Open areas can be photographed

throughout much of the year. Areas with sparse tree cover should be photographed during early spring (after grasses have emerged but before tree leaves have appeared) or late fall (after tree leaves have dropped). Areas of dense tree cover may be impossible to analyze using airphoto interpretation at any time.

An analysis of the photo characteristics of color, texture, site, and association, along with collateral soil information, is important for the identification of failing septic systems. Stereoscopic viewing is also important because it allows for the identification of slope, relief, and direction of surface drainage.

4.15 NATURAL DISASTER ASSESSMENT

Many forms of natural and human-induced disasters have caused loss of life, property damage, and damage to natural features. A variety of remote sensing systems can be used to detect, monitor, and respond to natural disasters, as well as assess disaster vulnerability. Here, we discuss wildfires, severe storms, floods, volcanic eruptions, dust and smoke, earthquakes, shoreline erosion, and landslides. NASA, NOAA, and the USGS maintain websites devoted to natural hazards (Appendix B).

Wildfires

Wildfires are a serious and growing hazard over much of the world. They pose a great threat to life and property, especially when they move into populated areas. Wildfires are a natural process, and their suppression is now recognized to have created greater fire hazards than in the past. Wildfire suppression has also disrupted natural plant succession and wildlife habitat in many areas.

Plate 11 shows a wildfire burning near the city of Los Alamos, New Mexico, as imaged by Landsat-7 (Chapter 6). Los Alamos is located on a series of mesas in the upper-right quadrant of the image. Plate 11*a* is a composite of bands 1, 2, and 3 (displayed as blue, green, and red, respectively), resulting in a “normal color” image. Plate 11*b* is a composite of bands 2, 4, and 7 (again displayed as blue, green, and red) and is a “false color image.” The normal color image shows the smoke plumes well but does not reveal much specific information about the areas that are burning at the time of image acquisition. In the false color image (*b*), the hottest actively burning areas appear bright red-orange in color, visible because of the large amount of energy emitted from the fires in the 2.08- to 2.35- μm wavelength sensitivity range of band 7 (Figure 2.22). The darker red and near-black-toned areas

are recently burned areas. The nearby darker green areas are unburned forest lands.

Severe Storms

Severe storms can take many forms, including tornados and cyclones. Tornadoes are rotating columns of air, usually with a funnel-shaped vortex several hundred meters in diameter, whirling destructively at speeds up to about 500 km/hr. Tornadoes occur most often in association with thunderstorms during the spring and summer in the midlatitudes of both the Northern and Southern Hemispheres. Cyclones are atmospheric systems characterized by the rapid, inward circulation of air masses about a low-pressure center, accompanied by stormy, often destructive, weather. Cyclones circulate counterclockwise in the Northern Hemisphere, and clockwise in the Southern Hemisphere. Hurricanes are severe tropical cyclones originating in the equatorial regions of the Atlantic Ocean or Caribbean Sea. Typhoons are tropical cyclones occurring in the western Pacific or Indian Oceans.

Tornado intensity is commonly estimated by analyzing damage to structures and then correlating it with the wind speeds required to produce such destruction. Tornado intensity is most often determined using the *Fujita Scale*, or *F-Scale* (Table 4.14). Although very few (about 2 percent) of all tornadoes reach F4 and F5 intensities, they account for about 65 percent of all deaths.

TABLE 4.14 Fujita Scale (F-Scale) of Tornado Intensity

F-Scale Value	Wind Speed (km/hr)	Tornado Intensity	Description of Damage	Examples
F0	64–116	Weak	Light	Branches broken, shallow-rooted trees pushed over
F1	117–181	Weak	Moderate	Surfaces peeled off roofs, mobile homes pushed off foundations or overturned
F2	182–253	Strong	Considerable	Roofs torn off frame houses, large trees snapped or uprooted
F3	254–332	Strong	Severe	Roofs and some walls torn off well-constructed houses, trains overturned, heavy cars lifted off ground and thrown
F4	333–418	Violent	Devastating	Well-constructed houses leveled, cars thrown.
F5	419–512	Violent	Incredible	Strong frame houses lifted off foundations and carried a considerable distance to disintegration, automobile-sized missiles flung through the air more than 100 m

Source: 2002 Encyclopedia Britannica online (<http://www.britannica.com>).

Plate 12 is a large-scale digital camera image showing a portion of the aftermath of an F4 tornado that struck Hayesville, Kansas. This tornado was responsible for 6 deaths, 150 injuries, and over \$140 million in property damage.

Plate 32 contains “before” and “after” Landsat-7 satellite (Chapter 6) images of the damage caused by an F3 tornado that struck Burnett County, Wisconsin. This storm resulted in 3 deaths, 8 serious injuries, complete destruction of 180 homes and businesses, and damage to 200 others. Figure 4.44 is a large-scale aerial photograph showing the “blowdown” of trees by this tornado. Tornado damage is also shown in Figure 8.31, a radar image of a forested area in northern Wisconsin.

Hurricane intensity is most often determined using the Saffir–Simpson Hurricane Scale, which rates hurricane intensity on a scale from 1 to 5, and is used to give an estimate of potential property damage and flooding along the coast from a hurricane landfall. The strongest hurricanes are “Category 5” hurricanes, with winds greater than 249 km/hr. Category 5 hurricanes typically have a storm surge 5.5 m above normal sea level (this value varies widely with ocean bottom topography) and result in complete roof failure on many residences, and some complete building failures. Many shrubs, trees, and signs are blown down. Severe and extensive window and door damage can occur, as can complete destruction of mobile homes. Also, there is typically major damage to the lower floors of all structures located less than 5 m above sea level and within 500 m of the shoreline. Before the 1940s, many hurricanes went undetected. At present every hurricane is detected and tracked by satellite imaging. Figure 4.45 is a MODIS satellite (Chapter 6) image of an offshore hurricane that peaked as a Category 5 hurricane. A typical hurricane structure can be seen, with a counterclockwise flow of air, and a center “eye,” with reduced wind speed and rainfall. Side-looking radar satellite images from Radarsat (Chapter 8) have also been used to monitor hurricanes.

Floods

Over-the-bank river flooding delivers valuable topsoil and nutrients to farmland and brings life to otherwise infertile regions of the world, such as the Nile River Valley. On the other hand, flash floods and large “100-year” floods are responsible for more deaths than tornadoes or hurricanes and cause great amounts of property damage.

Various examples of flooding can be found elsewhere in this book. Figure 4.24 is a multirate sequence of low altitude aerial photographs showing river flooding and its aftereffects. Figure 4.25 illustrates the appearance of a flooding river from a satellite perspective. Figures 4.26 and 4.27 illustrate new lakes formed by the overflow of the Nile River, again from a satellite perspective. And, Figure 8.48 shows flooding of Canada’s Red River as imaged by the Radarsat satellite.

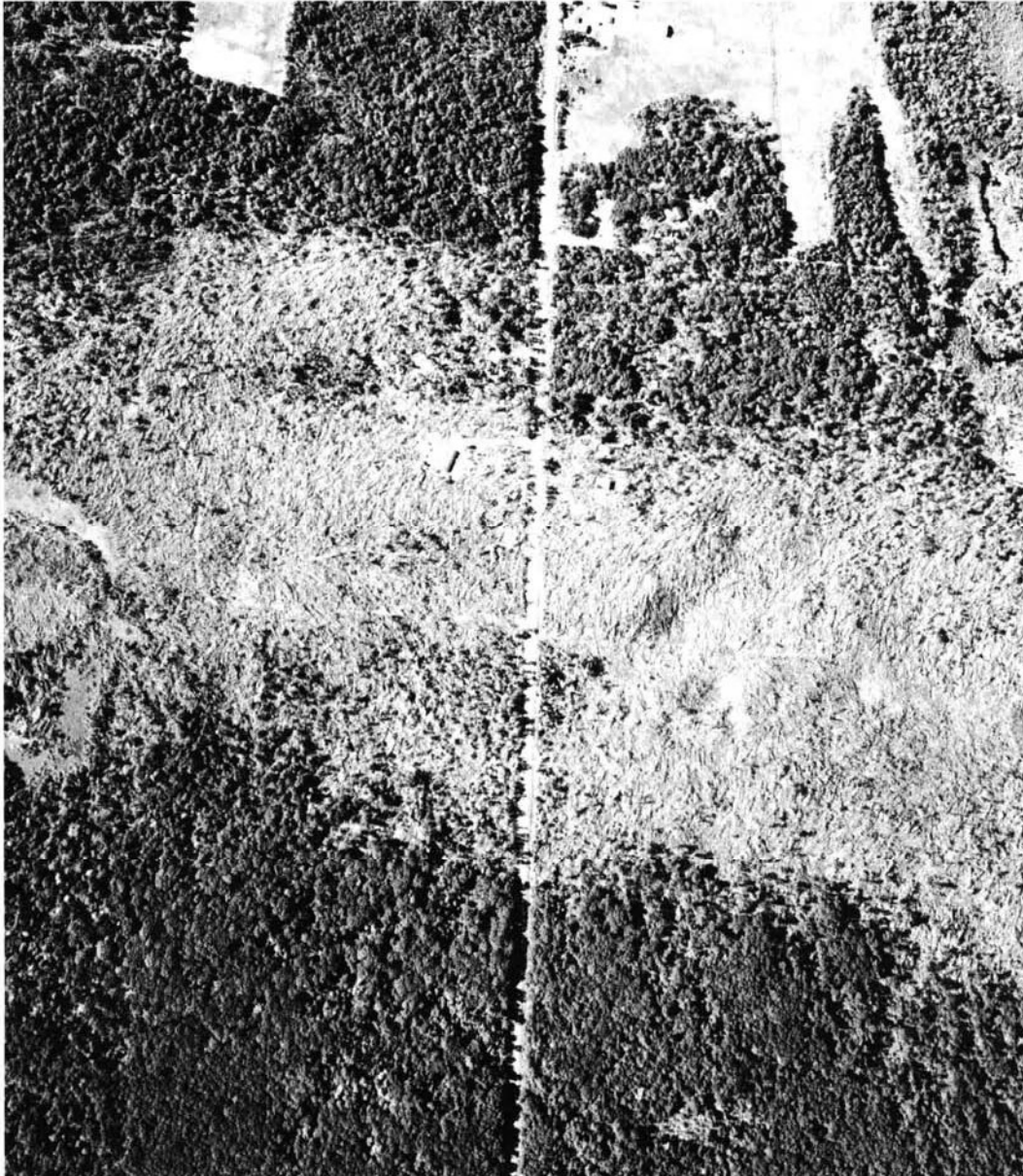


Figure 4.44 Aerial photograph showing the destruction of hundreds of trees by an F3 tornado that struck Burnett County, WI, on June 18, 2001. Scale 1:8100. (Courtesy Burnett County Land Information Office, University of Wisconsin-Madison Environmental Remote Sensing Center, and NASA Regional Earth Science Applications Center Program.)

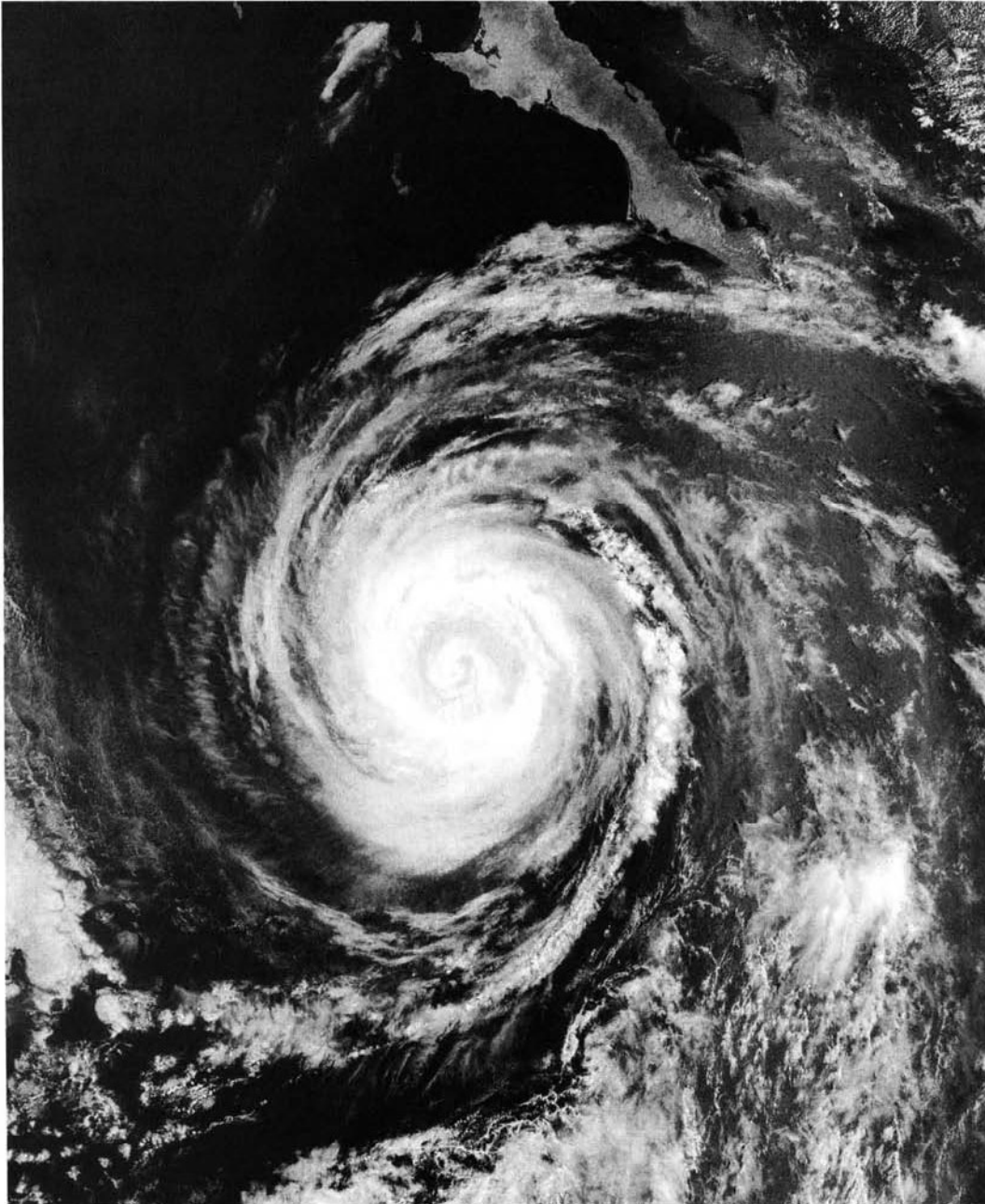


Figure 4.45 Hurricane Herman off Baja California, September 2, 2002, as imaged by MODIS. (Courtesy NASA.)

Volcanic Eruptions

Volcanic eruptions are one of earth's most dramatic and violent agents of change. Eruptions often force people living near volcanoes to abandon their land and homes, sometimes forever. Volcanic activity in the last 300 years has killed more than 250,000 people, destroyed entire cities and forests, and severely disrupted local economies. Volcanoes can present a major hazard to those who live near them, for a variety of reasons: (1) pyroclastic eruptions can smother large areas of the landscape with hot ash, dust, and smoke within a span of minutes to hours; (2) red hot rocks spewed from the mouth of a volcano can ignite fires in nearby forests and towns, while rivers of molten lava can consume almost anything in their paths as they reshape the landscape; (3) heavy rains or rapidly melting summit snowpacks can trigger lahars, sluices of mud that can flow for miles, overrunning roads and villages; and, (4) large plumes of ash and gas ejected high into the atmosphere can influence climate, sometimes on a global scale (from USGS and NASA Natural Hazards websites—see Appendix B).

Plate 38 shows an extensive volcanic terrain in central Africa. Numerous lava flows can be seen on the slopes of Nyamuragiro volcano, which dominates the lower portion of the image. To the upper right of Nyamuragiro volcano is Nyiragongo volcano, which erupted in 2002 with loss of life and great property damage in and around the city of Goma, located on the shore of Lake Kivu, which can be seen at the right edge of Plate 38.

Plate 13 is a Landsat-5 (Chapter 6) image showing the eruption of 3350-m-high Mt. Etna, Italy, Europe's most active volcano. The bright red-orange areas on the volcano's flanks are flowing lava and fissures containing molten lava. This image is a composite of Landsat bands 2 (sensitive to green energy), 5 (mid-IR), and 7 (mid-IR). In this color composite, band 2 is displayed as blue, band 5 as green, and band 7 as red. Because the molten lava emits very little energy in green wavelengths, and a great deal of energy in the mid-IR (Figure 2.22), it appears in Plate 13 with a red-orange color. (Note that Plate 4*b* showed flowing lava as photographed with color infrared film.) The bright, puffy clouds near the volcano were formed from water vapor released during the eruption. A thick plume of airborne ash can be seen blowing from the volcano, to the southeast (north is to the top of Plate 13).

Dust and Smoke

Aerosols are small particles suspended in the air. Some occur naturally, originating from volcanoes, dust storms, and forest and grassland fires. Human activities, such as the burning of fossil fuels, prescribed fires, and the alteration of natural land surface cover (e.g., slash-and-burn activities), also generate aerosols. Many human-produced aerosols are small enough to be inhaled,

so they can present a serious health hazard around industrial centers, or even hundreds of miles downwind. Additionally, thick dust or smoke plumes severely limit visibility and can make it hazardous to travel by air or road. Examples of smoke and volcanic ash can be seen in Plates 11 and 13, previously discussed.

Dust plumes have been observed in many arid regions around the globe. They can be extensive and travel great distances. For example, using satellite images, dust plumes originating near the west coast of Africa have been observed reaching the east coast of South America. Figure 4.46 shows an example of dust plumes over Baja California, blowing in a southwesterly direction, as imaged by the SeaWiFS satellite (Chapter 6).

Earthquakes

Earthquakes occur in many parts of the world and can cause considerable loss of life and property damage. Figure 4.11 illustrates extensive geologic features visible on satellite imagery that can be correlated with major geologic faults and major earthquake sites. Figure 6.29 shows the trace of ground cracks created during an earthquake that are clearly evident on a postearthquake satellite image. For information on earthquake hazards, see the USGS Earthquake Hazards Program website (Appendix B).

Shoreline Erosion

Driven by rising sea and lake levels, large storms, flooding, and powerful ocean waves, erosion wears away the beaches and bluffs along the world's shorelines. Bluff erosion rates vary widely, depending on geologic setting, waves, and weather. The erosion rate for a bluff can be regular over the years, or it can change from near zero for decades to several meters in a matter of seconds. Remote sensing studies of shoreline erosion have used a variety of platforms, from cameras in microlite aircraft to satellite data. Historical data using aerial photographs dating back to the 1930s, as well as more recent satellite data, can be used to document shoreline erosion over time. Also, recent studies of shoreline erosion have used Lidar data (Chapter 8).

Landslides

Landslides are mass movements of soil or rock down slopes and a major natural hazard because they are widespread. Globally, landslides cause an estimated 1000 deaths per year and great property damage. They commonly occur in conjunction with other major natural disasters, such as earthquakes,



Figure 4.46 Dust plumes over Baja California as imaged by the SeaWiFS satellite, February 2002. Scale 1:8,600,000. (Courtesy NASA.)

floods, and volcanic eruptions. Landslides can also be caused by excessive precipitation or human activities, such as deforestation or developments that disturb natural slope stability. They do considerable damage to infrastructure, especially highways, railways, waterways, and pipelines.

Historically, aerial photographs have been used extensively to characterize landslides and to produce landslide inventory maps, particularly because of their stereo-viewing capability and high spatial resolution. High resolution satellite data (Chapter 6), such as IKONOS, and the stereo data from SPOT-4, have proven useful for mapping large landslides, and the multi-incidence, stereo, and high resolution capabilities of Radarsat (Chapter 8) are also proving useful for landslide studies. Radar interferometry techniques (Chapter 8) have also been used in landslide studies in mountainous areas (Singhroy et al., 1998).

For additional information on landslide hazards, see the USGS Geologic Hazards—Landslides website (Appendix B).

4.16 PRINCIPLES OF LANDFORM IDENTIFICATION AND EVALUATION

Various terrain characteristics are important to soil scientists, geologists, geographers, civil engineers, urban and regional planners, landscape architects, real estate developers, and others who wish to evaluate the suitability of the terrain for various land uses. Because terrain conditions strongly influence the capability of the land to support various species of vegetation, an understanding of image interpretation for terrain evaluation is also important for botanists, conservation biologists, foresters, wildlife ecologists, and others concerned with vegetation mapping and evaluation.

The principal terrain characteristics that can be estimated by means of visual image interpretation are bedrock type, landform, soil texture, site drainage conditions, susceptibility to flooding, and depth of unconsolidated materials over bedrock. In addition, the slope of the land surface can be estimated by stereo image viewing and measured by photogrammetric methods.

Space limits the image interpretation process described to the assessment of terrain characteristics that are visible on medium-scale stereoscopic aerial photographs. Similar principles apply to nonphotographic and spaceborne sources.

Soil Characteristics

The term *soil* has specific scientific connotations to different groups involved with soil surveying and mapping. For example, engineers and agricultural soil scientists each have a different concept of soils and use a different terminology in describing soils. Most engineers consider all unconsolidated earth ma-